Biosensors and Bioelectronics 127 (2019) 221–228

Contents lists available at ScienceDirect

Biosensors and Bioelectronics

journal homepage: www.elsevier.com/locate/bios

An electrochemical aptasensor for staphylococcal enterotoxin B detection based on reduced graphene oxide and gold nano-urchins

Somayeh Mousavi Nodoushan[a], Navid Nasirizadeh[b,*], Jafar Amani[a], Raheleh Halabian[a], Abbas Ali Imani Fooladi[a,*]

[a] Applied Microbiology Research Center, Systems Biology and Poisonings Institute, Baqiyatallah University of Medical Sciences, Tehran 14359-44711, Iran
[b] Department of Textile and Polymer Engineering, Yazd Branch, Islamic Azad University, Yazd 8916871967, Iran

ARTICLE INFO

Keywords:
Staphylococcal enterotoxin B
Electrochemical biosensor
Aptasensor
Reduced graphene oxide
Gold nano-urchins

ABSTRACT

Detection of staphylococcal enterotoxin B (SEB) as a bacterial toxin causing severe food poisoning is of great importance. Herein, we developed an electrochemical aptasensor for SEB detection using a screen printed electrode modified with reduced graphene oxide (rGO) and gold nano-urchins (AuNUs). Afterward, the single-stranded DNA probe was attached to the surface of AuNUs on the modified electrode and then the specific aptamer was attached to the probe. In the presence of SEB molecules, the aptamer detached from the electrode surface and after applying the electrochemical signal generator, hematoxylin and the peak current of differential pulse voltammetry (DPV) were recorded. Due to the intercalation mechanism of hematoxylin-DNA interaction, the detachment of aptamer from electrode surface decreased the DPV peak current and the calibration graph (peak current vs SEB concentration) can be used for quantification of SEB. The cyclic voltammetry (CV) and electrochemical impedance spectroscopy (EIS) and also field emission scanning electron microscope imaging were used for electrode characterization. Selectivity experiments of the developed aptasensor showed a very distinct difference between SEB and other nonspecific molecules. A wide linear range from 5.0 to 500.0 fM was achieved and the detection limit was calculated as 0.21 fM. The performance of the aptasensor was checked in spiked food samples as simulated real samples and the results showed no significant difference compared to the synthetic samples. Results of selectivity and repeatability of the aptasensor were satisfactory. In addition, better recovery percentages and also lower standard deviation of aptasensor compared to a commercial ELISA kit of SEB detection proved the superior performance of the proposed aptasensor.

1. Introduction

One of the most common foodborne pathogens worldwide is *Staphylococcus aureus* that produces a variety of virulence factors like enzymes and toxins including enterotoxin, neurotoxin and cytotoxin which could be harmful to our health (DeGrasse, 2012; Fooladi et al., 2010; Mello et al., 2016; Saadat et al., 2014; Wu et al., 2016). A wide range of enterotoxins are secreted by enterotoxigenic strains of the *Staphylococcus aureus* (Deng et al., 2014; Hedayati et al., 2016; Huang et al., 2015; Imani-Fooladi et al., 2014; Salmain et al., 2011; Wu et al., 2013; Zargar et al., 2014; Zeleny et al., 2015). Among these toxins, the staphylococcal enterotoxin B (SEB) is a bit different due to its super-antigenic properties in nature, leading to immunosuppression and serious food poisoning via the consumption of contaminated food like dairy, salads, unrefrigerated meats and also bakery products (Fooladi et al., 2009; Gholamzad et al., 2015; Imani Fouladi et al., 2011; Wu et al., 2013). Gastrointestinal symptoms produced by SEB are including but not limited to nausea, vomiting, and diarrhea. Moreover, this toxin could also be transmitted through the respiratory tract and thereby be categorized as a biological weapon (Wu et al., 2016, 2013; Yang et al., 2009).

Researchers have found that lethal dose of SEB is 20 ng/kg and at lower concentrations can cause disability in humans. Therefore, the detection of this toxin in low concentrations in food is very important (Chrouda et al., 2013; Deng et al., 2014). Conventional detection methods for SEB consist of bioassay methods, polymerase chain reaction (PCR), liquid chromatography-mass spectrometry (LC-MS) and enzyme-linked immunosorbent assay (ELISA). Most of these detection strategies are expensive, time-consuming as well as requiring complicated instruments and trained personnel (Deng et al., 2014; Hedayati et al., 2016; Huang et al., 2015).

In contrast to the above techniques, the electrochemical biosensors

* Corresponding authors.
E-mail addresses: nasirizadeh@iauyazd.ac.ir (N. Nasirizadeh), imanifouladi.a@bmsu.ac.ir (A.A. Imani Fooladi).

https://doi.org/10.1016/j.bios.2018.12.021
Received 21 October 2018; Received in revised form 9 December 2018; Accepted 10 December 2018
Available online 16 December 2018
0956-5663/

and/or aptasensors have some potential to be more suitable for SEB detection and have become one of the most popular SEB detection methods due to their efficient advantages, low-cost, easy-to-use and sensitive quantification (Azimzadeh et al., 2015; Hajihosseini et al., 2016; Justino et al., 2015; Nasirizadeh et al., 2011; Shoaie et al., 2018a; Shojaei et al., 2016; Wu et al., 2016; Yazdanparast et al., 2018).

Various electrochemical techniques and strategies, sometimes along with signal amplification strategies have been used in electrochemical biosensing systems so far and most of them have used nanomaterials and nanostructures to achieve better sensitivity throughout different ways and reasons (Azimzadeh et al., 2017; Seifati et al., 2018; Shoaie et al., 2018a, 2018b; Syedmoradi et al., 2017). In the past decade, the aptamer-based biosensors, namely aptasensors, which use aptamer as their detection agent, have gained great attention; because they can recognize their specific ligands and bind to different targets with high affinity and specificity (Deng et al., 2014; Luo et al., 2014; Radi, 2011). Aptamers present many significant advantages in contrast with antibodies including low immunogenesis, chemical permanence, low molecular weight and high affinity (Radi, 2011; Topkaya and Azimzadeh, 2016).

Electrochemical biosensors and nanobiosensors have been used for SEB detection, previously. Different approaches recruit different receptors such as aptamers (Xiong et al., 2018), antibodies (Chatrathi et al., 2007) and also different nanomaterials such as composites of graphene and gold nanoparticles (Sharma et al., 2016), platinum nanoparticles (Sharma et al., 2014), carbon nanotubes (Tang et al., 2010) for the detection of SEB. But, as far as we know, the combination of the two nanomaterials including reduced graphene oxide (rGO) and gold nano-urchins (AuNUs) was not applied in any reported study on SEB detection. The rGO has been used in different electrochemical biosensors and aptasensors so far and it has been reported that the high conductivity and high surface area of rGO make it a good choice for electrochemical methods (Chen et al., 2010; Pumera, 2010, 2011; Zhou et al., 2009). The AuNU is a special type of gold nanoparticle with a higher surface area that can provide a bigger surface for probe attachment (Aghili et al., 2017; Chiwunze et al., 2017; Sabri et al., 2016; Thapliyal et al., 2017).

In the current study, we developed an electrochemical aptasensor adopting DNA hybridization by the self–assembled monolayer (SAM) technique for SEB detection. We have used a specifically designed aptasensor with high affinity to target SEB toxin molecules. In addition, we have used the combination of rGO and AuNUs on the working electrode to enhance the sensitivity of the aptasensor. The specific conjugation probe which is partly complementary to the aptamer linker was used to attach aptamers through a linker to the gold nano-urchins. It has to be mentioned that such a combination of nanomaterials has not been found by searching the literature for electrochemical biosensing; therefore, it is the first study of its kind in this field.

2. Experimental

2.1. Chemicals and solutions

All the chemicals used to prepare solutions were applied without further purification as purchased from either Merck Company or Sigma-Aldrich Company, based on their availability. The gold nano-urchins (AuNUs) (average size 60 nm, Cat. No. 795399) and chemically reduced graphene oxide (rGO) (Cat. No. 777684) were achieved from Sigma-Aldrich Co. (USA). All the solutions were prepared using double distilled (DDW) water and their making protocols were based on the previous publications from our research team (Azimzadeh et al., 2017, 2016; Hajihosseini et al., 2016). All solutions and glassware were sterilized using the autoclave.

2.2. Oligonucleotides

The sequence of SEB aptamer was obtained from a previous SELEX study of our research team (Hedayati et al., 2016). All oligonucleotides were synthesized, HPLC-purified and received in lyophilized form by Metabion Company (Germany) with the following sequences:

Aptamer SEB: 5′-TGCAGGATCCGGTATCCGTGCACACACACCCAAC AACCAGCTGCCGCACCGGAGGAATTCTCGT-3′

ssProbe: 5′-Thiol- TTTTTTACGAGAATTCCTCCGGTGCG-3′.

2.3. Electrochemical instrumentation

Electrochemical measurements, including cyclic voltammetry (CV), differential pulse voltammetry (DPV) and electrochemical impedance spectroscopy (EIS) were performed with Autolab potentiostat/galvanostat PGSTAT30 from Metrohm Company (Netherland) at laboratory temperature (25 ± 1 °C). The interface program was GPES version 4.9 and screen-printed carbon electrode (SPCE) from DropSens Company (Spain) was used instead of conventional three electrode system. The working electrode of the SPCE was made of carbon (4 mm diameter), the counter electrode was made of platinum and the reference electrode was made of silver.

2.4. Preparation of aptasensor

In this section, all the parameters used for the preparation of the aptasensor have been optimized through the separate experiments which their results are shown in the Supplementary text. In addition, the concentration of rGO and AuNUs are obtained from the previous work (Aghili et al., 2017). To prepare the aptasensor, first 2.0 µL of 1.0 mg mL^{-1} rGO solution was dropped onto the surface of the working electrode and then slowly dried at room temperature. At this stage, 2.0 µL of AuNU solution at a concentration of 100.0 µg mL^{-1} was dropped onto the surface of rGO/SPE and was kept at ambient temperature to be dried slowly. Afterward, 2.0 µL droplet of the immobilization buffer solution containing 80.0 nM of the thiolated single-strand probes was deposited on the modified electrode surface and for the attachment of the probes onto the gold nano-urchins surface, incubated in a high-humidity container at room temperature for 100 min. After washing with the washing solution, the electrode was immersed in 0.1 mM MCH solution for 5 min to block the remaining bare regions on the surface of AuNUs.

The resulting modified electrode was rinsed with (80:20 v/v) ethanol: water and distilled water, respectively. In the end, the prepared electrode was immersed in the hybridization buffer solution (pH 7.0) containing 1100.0 fM concentration of the aptamer at room temperature (25 ± 1 °C) for 120 min. Finally, in this step, the aptasensor was ready. Then the aptasensor was incubated with the desired concentrations of the SEB for 125 min.

To evaluate accurate modifications on the working electrode during the fabrication process, after every preparation, the analysis of CV and EIS was carried out in the solution of 5.0 mM $K_3[Fe(CN)_6]/K_4[Fe(CN)_6]$ containing 1.0 M KCl. The potential range of CV was − 0.025 to 0.33 V with a sweep rate of 0.02 V s^{-1} and EIS was performed from 100 kHz to 0.01 Hz with amplitude of 5 mV and potential of 0.27 V. Additionally, the electrochemical signal measurements were done using differential pulse voltammetry (DPV), with a modulation time of 0.05 s, amplitude of 25 mV and step potential of 50 mV in 0.1 mol L^{-1} PBS buffer (pH 7.0).

2.5. Hematoxylin accumulation on the aptasensor

The obtained aptasensor was immersed in the 0.1 mM phosphate buffer solution (pH 7.0) containing 0.09 mM of hematoxylin for 10 min stirring at low speeds. After that, the electrode was rinsed with a washing solution for 10 S. In order to create a control, once the

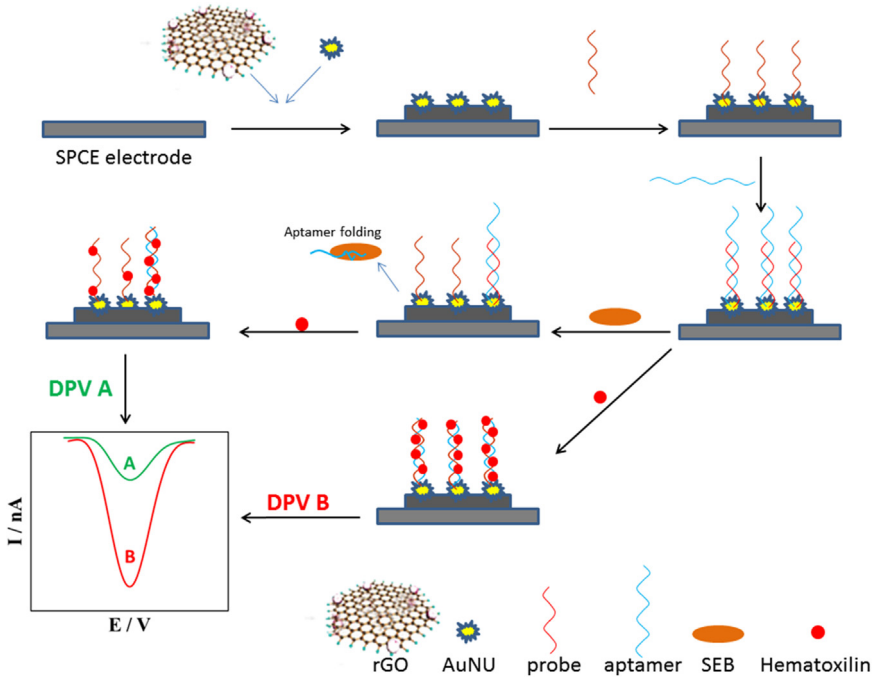

Scheme 1. Schematic review of fabrication process of SEB aptasensor using reduced graphene oxide and gold nano-urchins.

aptasensor was prepared, the electrode was immersed in the hematoxylin solution without applying the SEB solution and the peak current of DPV was compared between these cases and current difference was calculated.

2.6. Scanning electron microscope (SEM) analysis

The SEM imaging analysis of the working electrode surface was performed using field emission scanning electron microscopy (FE-SEM) Zeiss Sigma 500 VP (Germany).

3. Results and discussion

Preparation of the nanobiosensing mechanism of the SEB based on an electrochemical aptasensor is reviewed in a Scheme 1 for the better explanation. As it can be seen in this scheme, the main working mechanism is based on detachment of the aptamer in the presence of the SEB toxin. In general, preparation of the electrode started with modification of the SPCE with rGO and AuNUs and consequently with specific probe that is partially hybridized with a segment of aptamer. After the introduction of the toxin, the affinity of the SEB molecule towards its specific aptamer, makes the aptamer detached from the surface of the modified electrode. This leads to a decrease in DPV signal of the electrochemical label, hematoxylin. This is caused by the intercalation interaction of hematoxylin with DNA that means preference towards double-stranded DNA (probe + aptamer) compared to the single-stranded DNA (just probe). The peak current difference then will be calculated and its relationship to the amount of SEB is presented in the calibration graph.

3.1. Characterization by cyclic voltammetry

After each assembly step, cyclic voltammetry can give useful information on the changes of the electrode behavior. The cyclic voltammograms of the electrode in 1.0 mM $K_3[Fe(CN)_6]$ solution for bare SPE electrode, SPE/rGO, AuNUs/rGO/SPE, ssDNA/AuNUs/rGO/SPE, MCH/ssDNA/AuNUs/rGO/SPE and dsDNA/AuNUs/rGO/SPE are shown in Fig. 1A. As it is presented, a high peak current voltammogram was obtained by using nanomaterials like rGO and gold nano–urchins,

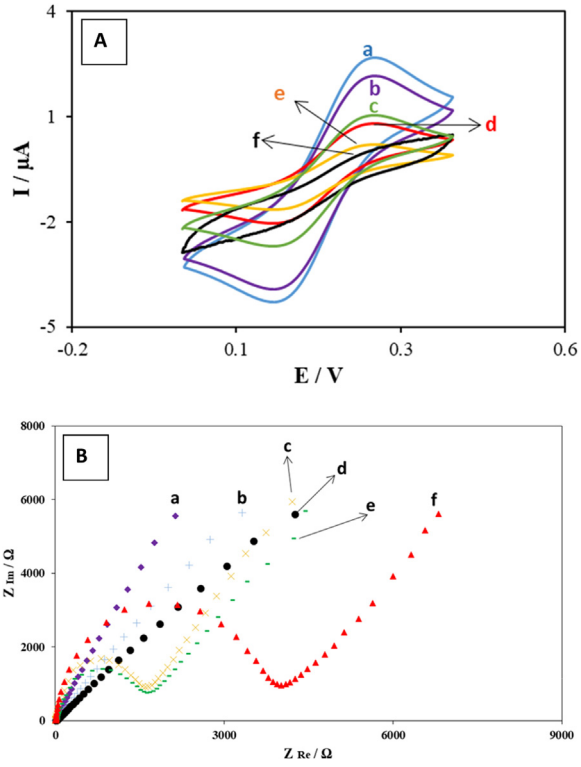

Fig. 1. (A) The cyclic voltammograms of the modified SPE electrode in the $K_3[Fe(CN)_6]$ solution after every step of the aptasensor fabrication. (a) AuNUs/rGO/SPE, (b) SPE/rGO, (c) MCH/ssDNA/AuNUs/rGO/SPE, (d) ssDNA/AuNUs/rGO/SPE, (e) bare SPE electrode and (f) dsDNA/AuNUs/rGO/SPE. **(B)** The Nyquist plot of the different modified SPE electrodes in the solution of 5.0 mM $K_3[Fe(CN)_6]$ containing 1.0 M KCl. (a) AuNUs/rGO/SPE, (b) SPE/rGO, (c) MCH/ssDNA/AuNUs/rGO/SPE, (d) bare SPE electrode, (e) ssDNA/AuNUs/rGO/SPE and (f) dsDNA/AuNUs/rGO/SPE.

because they have very high electron conductivity. Following immobilization of the SS-probe and MCH treatment on the SPE surface, the current dramatically decreased due to the blockage of the electrode surface by the SS-probes and MCH molecules (curve b). After hybridization of the SS-probe with the target DNA, the redox peak currents declined significantly (curve d) because, the hybridized oligonucleotides accumulate on the SPE surface which is negatively charged. Likewise, they cause extra blocking layer for the electron transfer of the $K_3[Fe(CN)_6]$ onto the SPE surface.

3.2. Characterization by EIS

In addition to CV analysis, the EIS measurements were also performed on the modified electrode after every modification step. The resulted Nyquist plot of this section is represented in the Fig. 1B. By comparing the EIS curves that are associated with a working electrode modification, we can assess the electrochemical behavior of each modification step, same as the CV analysis explained in the previous section. Thus, it can be concluded here, the curve d is for bare SPCE electrode and its resistance was decreased when the rGO was added to the electrode surface (curve b) and further decrease happened after adding the AuNUs to the electrode (curve a). But, after adding the ssProbe on the AuNUs, the resistance became higher, due to the spatial blocking of the anions/cations to reach the electrode surface and also the repellant effect of the DNA strand because of their negative charge (curve e). After applying the MCH, the resistance decreased (curve c) and after hybridization of the aptamer to the ssProbe the resistance increased again (curve f) and reached its higher value in the plot. It can be explained in the same way as when applying the ssProbe on the AuNUs, considering the negative charge of the DNA strand which now is higher due to the double stand structure of the hybridized aptamer-ssProbe and also the spatial blockage of the ions to reach the electrode surface is more.

3.3. Characterization by SEM

SEM imaging is a proper way to observe the correct assembling procedure of the nanomaterials on the working electrode surface. The SEM imaging was performed for the modified electrode surface after changing with reduced graphene oxide (Fig. 2A) and also after adding gold nano-urchins on the surface of reduced graphene oxide (Fig. 2B). The presence of graphene oxide layer on the electrode surface is presented appropriately in the Fig. 2A. Furthermore, in the Fig. 2B the suitable distribution of the gold nano-urchins on the graphene oxide layer is shown. The results of SEM imaging were proved the suitable decoration of the rGO and AuNUs on the modified electrode surface and this protocol was selected for the rest of the study. Therefore, the probe immobilization and further modifications on the electrode surface was performed based on the modification protocol of rGO and AuNUs.

3.4. Analytical performance and selectivity of the nanobiosensor

To evaluate the selectivity of SEB toxin attachment on the modified SPCE electrode with the aptamer on the rGO and AuNUs layer, the selectivity test was performed. The DPVs of hematoxylin accumulated on the modified SPE after hybridization with 2.0 μmol L^{-1} solution of specific and non-specific toxins are measured for four replications (error bar represented in the graph) and comparison of their peak current are shown in Fig. 3A. Due to the working mechanism of the aptasensor, the lower peak currents are desirable and show the high sensitivity of the nanobiosensing mechanism. As it can be seen in the Fig. 3A, the peak current of SEB attached to aptasensor was very lower than the peak current of control, staphylococcal enterotoxin C (SEC), staphylococcal enterotoxin A (SEA), bovine serum albumin (BSA) and the blank solution which are similar to each other, with very higher current compared to the SEB toxin. From these results, the high

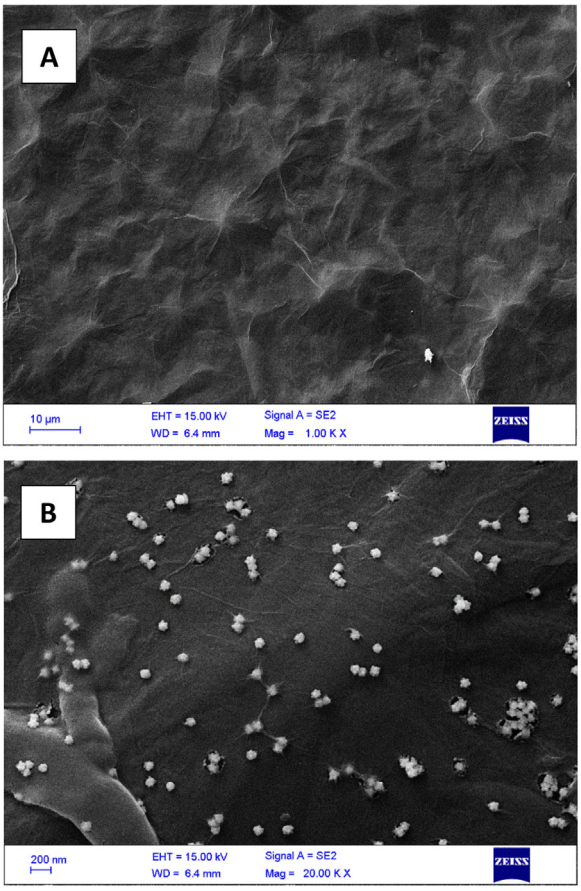

Fig. 2. SEM images of the (A) rGO and (B) rGO/AuNUs modified SPE electrode.

selectivity of the aptasensor to the SEB in comparison with other non-specific toxins and proteins was concluded and this could be due to the high affinity of the designed aptamer to the SEB toxin.

Additionally, the analytical performance of the aptasensor was tested by different concentrations of the SEB and the resulted DPVs were recorded for four replications. Based on the evaluations completed in this part of the study, there are 10 different concentrations of SEB that do have a linear relationship with the peak current and can be showed as linear range or dynamic range of the aptasensor. These 10 peaks and also the calibration curve of the study are shown in the Fig. 3B. According to the calibration curve, the concentrations of SEB were in a linear relationship with the peak current in the range of 5.0–500.0 fM which is called the linear range or dynamic range. Based on the formula explained earlier in the previous publications, the detection limit was calculated for the aptasensor to be 0.21 fM of SEB.

The reproducibility of the aptasensor was also tested through a set of experiments that repeated the detection process of the SEB in a distinct amount by the aptasensor. In this section, the five replications were performed by the fabricated aptasensor to detect the 20.0 fM concentration of the SEB and the results showed only 5.4% of relative standard deviation around the mean current of five replication. Such a low standard deviation could reveal the reproducibility of the aptasensor.

The performance of the aptasensor is compared to other previously published works about the detection of SEB and shown in the Table 1. By achieving a very low detection limit and also wide linear range, the reported aptasensor is better in sensitivity compared to the most of the previously studied SEB sensors with different detection methods and strategies that are reported in Table 1. This might be originated from the fact that we used the combination of the two nanomaterials rGO with high conductivity and high surface area for the attachment of

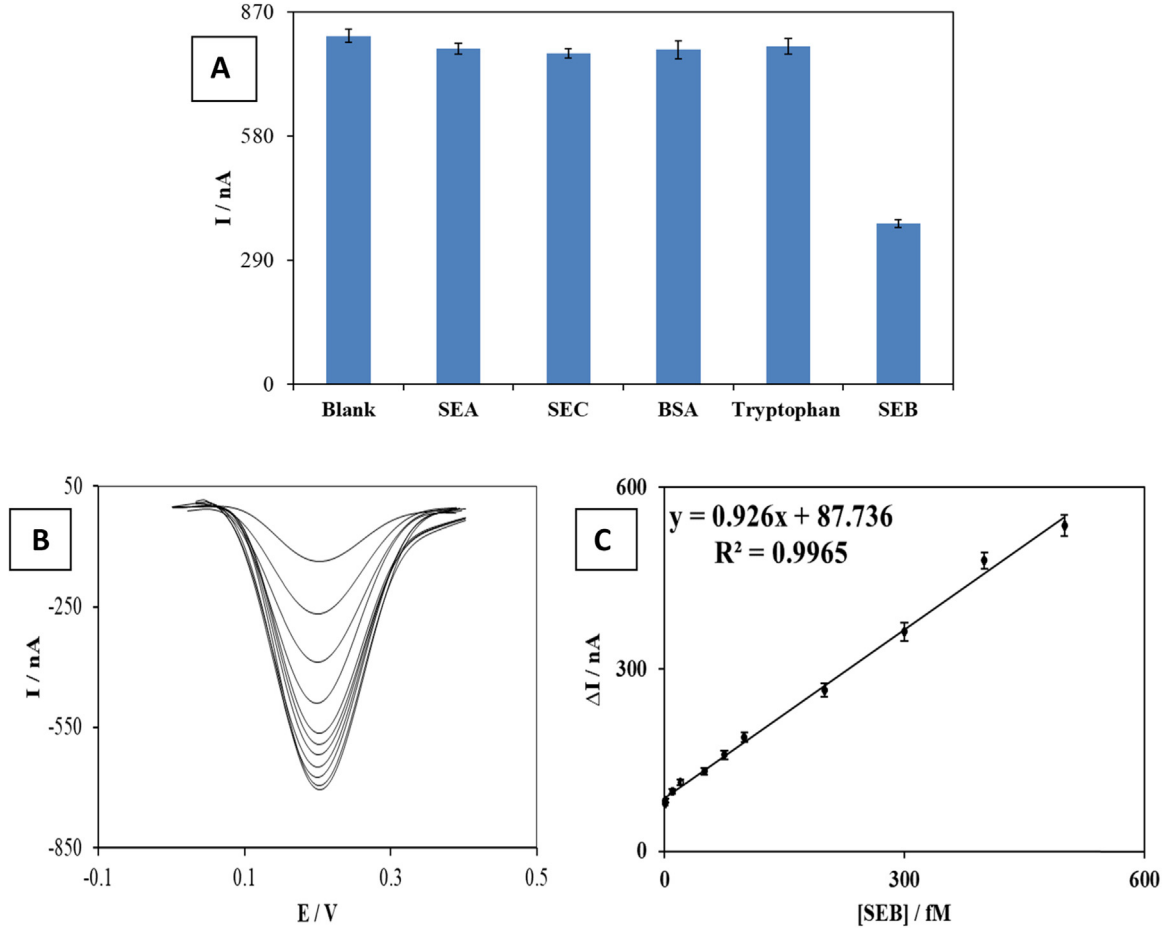

Fig. 3. (A) Results of the selectivity of the aptasensor in different solutions containing specific target toxin (SEB) and other non-specific molecules SEA, SEC, BSA and also a solution without any sample designated blank. **(B)** DPVs of the linear range of the aptasensor and **(C)** calibration curve and corresponding function (with error bars of three replications).

AuNUs and also the AuNUs itself with very high surface area compared to regular spherical gold nanoparticles. Optimization experiments to achieve better results for the aptasensor to detect SEB are also another probable reason in this regard.

3.5. Performance in the simulated real sample

Performance of each detection method should be evaluated in the real sample to be used in actual clinical studies. For this reason, the aptasensor was assessed further in simulated samples by spiking an

Table 1
Comparison of the aptasensor parameters and functions to previous publications for SEB detection.

Mechanism	Detection limit	Linear range	Ref.
Fluorescence	0.3 pg mL^{-1}	0.001–1.0 ng mL^{-1}	(Wu et al., 2013)
Fluorescence	0.069 pg mL^{-1}	0.10–9.0 ng mL^{-1}	(Huang et al., 2015)
Chemiluminescence	0.01 ng mL^{-1}	–	(Yang et al., 2009)
Immunosorbent	0.01 ng mL^{-1}	0.01–10.0 ng mL^{-1}	(Schotte et al., 2002)
Piezoelectric	0.1 ng mL^{-1}	–	(Gao et al., 2000)
Mass spectrometry	1.0 ng mL^{-1}	–	(Nedelkov and Nelson, 2003)
Mass spectrometry	3.0 pmol mL^{-1}	–	(Kientz et al., 1997)
Surface Plasmon Resonance	0.05 fM	–	(Gupta et al., 2010a)
Surface Plasmon Resonance	10.0 ppb	10.0–1000.0 ng g^{-1}	(Rasooly, 2001)
Surface Plasmon Resonance	2.5 ppb	–	(MEDINA, 2003)
Surface Plasmon Resonance	1.0 ng mL^{-1}	1.0–40.0 ng mL^{-1}	(Medina, 2006)
Surface Plasmon Resonance	1.0 pM	2.0–32.0 pM	(Gupta et al., 2010b)
Electrochemical	0.17 ng mL^{-1}	0.5–500.0 ng mL^{-1}	(Xiong et al., 2018)
Electrochemical	10.0 ng mL^{-1}	0.1–1000.0 ng mL^{-1}	(Sharma et al., 2016)
Electrochemical	1.0 ng mL^{-1}	1.0 ng/mL to 1.0 μg/mL	(Sharma et al., 2014)
Electrochemical	0.24 ng mL^{-1}	2.0–512.0 ng mL^{-1}	(Deng et al., 2014)
Electrochemical	–	10.0–35.0 fM	(Tang et al., 2010)
Quartz Crystal Microbalance	2.25 ng/mL	0.1–1000 μg/mL	(Liu et al., 2014)
Fluorescent	1.6 ng/mL	–	(Spindel et al., 2015)
Electrochemical	0.21 fM	5.0–500.0 fM	This work

Table 2
Results of the study of (A) the aptasensor function in the simulated real food samples with three spiked concentrations of SEB and (B) a commercial kit function on the simulated real food samples for six different spiked concentrations of SEB.

(A) Aptasensor function in simulated real samples

Sample	Spiked SEB (fM)	Quantified after spiking (fM)	Recovery percentage (%)	Relative standard deviation (RSD) (%)
Milk	10.0	10.2	102.0	3.12
	40.0	39.7	99.2	3.44
	500.0	501.9	100.3	4.98
Meat	10.0	9.4	94.0	3.31
	40.0	41.1	102.7	4.23
	500.0	504.5	100.9	4.18
Human serum	10.0	9.8	98.0	2.94
	40.0	40.9	102.2	5.33
	500.0	497.6	99.5	4.45

(B) Commercial ELISA kit function in the real sample study

Sample	Reference concentration (ng mL^{-1})	Detected by kit (ng mL^{-1})	Recovery percentage (%)	Coefficient of variation (CV) (%)
Milk	0.16	0.135	84.37	7.4
	0.3	0.24	80	14.1
	0.63	0.50	79.36	7.4
	1.25	1.11	88.8	7.2
	2.5	2.007	80.28	4.78
	5.0	3.89	77.1	6.9
Meat	0.16	0.14	87.5	5.71
	0.3	0.27	90	3.03
	0.63	0.47	74.6	8.08
	1.25	0.97	77.6	5.15
	2.5	2.02	80.8	6.93
	5.0	3.87	77.4	6.46
Human serum	0.16	0.13	81.25	6.7
	0.3	0.26	86.66	11.3
	0.63	0.61	96.82	5.8
	1.25	1.18	94.4	7.2
	2.5	2.19	87.6	5.5
	5.0	4.56	91.2	6.4

exact amount of SEB toxin in three different samples including two food samples (milk and meat extract) and also human serum sample. The samples were read by the aptasensor before spiking the SEB and then again after spiking of different concentrations of the SEB. In four replications the mean recovery percentage and also the relative standard deviation (RSD) were calculated for each spiked concentration in each sample. The results are shown in the Table 2A. As it is clear, the recovery percentages are near to 100% with low RSD percentage that shows the repetitive results of the aptasensor in real sample and also good recovery percentage without any significant interfering effect from non-specific moieties and molecules in the real samples of milk, meat and human serum. This is a very important specification for each detection test in lab experiment and shows the performance of the method in real samples. Therefore, this result could be a reason to suggest performing real clinical studies of SEB quantification using this aptasensor in detection labs.

3.6. Confirming with a commercial kit

To confirm the aptasensor results in the previous section which were simulated real samples, an experiment was done by using a commercial staphylococcal enterotoxin B (SEB) detection kit (Cat No. 6030) from Chondrex Inc. (USA) following the protocols of the manufacturer. Because of the different linear range of the commercial kit (0.16–10.0 ng/mL) some concentrations that were tested with the aptasensor could not be measured using the commercial kit because they were lower than its detection limit. The commercial ELISA kit was used to measure the three concentrations of the SEB in three replications spiked into the human serum, milk and meat. The results of the experiments in this part are shown in the Table 2B demonstrating the recovery percentage of each experiment and their respective coefficient of variation (CV) percentages for three replications.

The standard samples which were provided by the manufacturer were also tested to assure the function of the detection kit. However, it has to be mentioned that the function of the ELISA kit in the standard sample solutions was much more accurate than the provided real samples of foods and serum, which is reflected in the results of the kit represented in the Table 2B. As it is revealed the standard deviation of the ELISA kit is higher than the fabricated aptasensor and could be another reason to consider this aptasensor for clinical applications of SEB detection. In addition, another advantage of this biosensor is that its detection limit is very lower than the commercial kit. Therefore, the only concentrations of the SEB in the linear range of commercial kit could be tested by the aptasensor.

4. Conclusion

The developed electrochemical aptasensor showed high sensitivity for staphylococcal enterotoxin B (SEB) in milk, meat and serum samples. Role of reduced graphene oxide (rGO) and gold nano-urchins (AuNUs) and also screen-printed electrode (SPCE) seems important in this regard. In addition, high selectivity of aptasensor towards SEB in comparison with the non-specific molecules that is provided by specific conjugation of aptamer-SEB molecule provides extra advantages for the developed system. Results in simulated real samples were also favorable to be applied in future for real food samples. Although there are some limitations and challenges left to be considered on the road to commercialization. The stability of the method should be enhanced to be more adaptable for storage and be used in every condition. But, on the other hand, the low-cost and simple production of the aptasensor is of great importance, especially in the commercialization of the product. Furthermore, the comparison of the results with a commercial detection kit of SEB showed that the standard deviations of the aptasensor measurements are much lower than a commercial ELISA kit which is used regularly in this field. It can be suggested that the application of a portable potentiostat/galvanostat in related future works will provide an extra advantage for the aptasensor because it can be used as a point-of-care device to assess food samples in the field instead of advanced laboratories.

CRediT authorship contribution statement

Somayeh Mousavi Nodoushan: Conceptualization, Investigation, Writing - original draft, Visualization. **Navid Nasirizadeh:** Conceptualization, Methodology, Writing - review & editing, Supervision. **Jafar Amani:** Methodology, Resources. **Raheleh Halabian:** Methodology, Resources. **Abbas Ali Imani Fooladi:** Conceptualization, Methodology, Writing - review & editing, Supervision, Resources.

Acknowledgements

This research is a part of Somayeh Mousavi Nodoushan's doctoral dissertation. Authors are thankful for all the supports and funding from the *Applied Microbiology Research Center, Systems Biology and Poisonings Institute,* Baqiyatallah University of Medical Sciences and Yazd Branch, Islamic Azad University, Iran. Authors kindly acknowledge the professional service of Dr. Mojtaba Hedayati.

Appendix A. Supplementary material

Supplementary data associated with this article can be found in the online version at doi:10.1016/j.bios.2018.12.021.

References

Aghili, Z., Nasirizadeh, N., Divsalar, A., Shoeibi, S., Yaghmaei, P., 2017. A nanobiosensor composed of exfoliated graphene oxide and gold nano-urchins, for detection of GMO products. Biosens. Bioelectron. 95, 72–80.

Azimzadeh, M., Nasirizadeh, N., Rahaie, M., Naderi-Manesh, H., 2017. Early detection of Alzheimer's disease using a biosensor based on electrochemically-reduced graphene oxide and gold nanowires for the quantification of serum microRNA-137. RSC Adv. 7 (88), 55709–55719.

Azimzadeh, M., Rahaie, M., Nasirizadeh, N., Ashtari, K., Naderi-Manesh, H., 2016. An electrochemical nanobiosensor for plasma miRNA-155, based on graphene oxide and gold nanorod, for early detection of breast cancer. Biosens. Bioelectron. 77, 99–106.

Azimzadeh, M., Rahaie, M., Nasirizadeh, N., Naderi-Manesh, H., 2015. Application of Oracet blue in a novel and sensitive electrochemical biosensor for the detection of microRNA. Anal. Methods 7 (22), 9495–9503.

Chatrathi, M.P., Wang, J., Collins, G.E., 2007. Sandwich electrochemical immunoassay for the detection of Staphylococcal Enterotoxin B based on immobilized thiolated antibodies. Biosens. Bioelectron. 22 (12), 2932–2938.

Chen, D., Tang, L., Li, J., 2010. Graphene-based materials in electrochemistry. Chem. Soc. Rev. 39 (8), 3157–3180.

Chiwunze, T.E., Thapliyal, N.B., Palakollu, V.N., Karpoormath, R., 2017. A simple, efficient and ultrasensitive gold nanourchin based electrochemical sensor for the determination of an antimalarial drug: mefloquine. Electroanalysis 29 (9), 2138–2146.

Chrouda, A., Braiek, M., Rokbani, K.B., Bakhrouf, A., Maaref, A., Jaffrezic-Renault, N., 2013. An immunosensor for pathogenic staphylococcus aureus based on antibody modified aminophenyl-Au electrode. ISRN Electrochem. 2013.

DeGrasse, J.A., 2012. A single-stranded DNA aptamer that selectively binds to Staphylococcus aureus enterotoxin B. PLoS One 7 (3), e33410.

Deng, R., Wang, L., Yi, G., Hua, E., Xie, G., 2014. Target-induced aptamer release strategy based on electrochemical detection of staphylococcal enterotoxin B using GNPs-ZrO_2-Chits film. Colloids Surf. B: Biointerfaces 120, 1–7.

Fooladi, A.A., Sattari, M., Nourani, M.R., 2009. Study of T-cell stimulation and cytokine release induced by Staphylococcal enterotoxin type B and monophosphoryl lipid A. Arch. Med. Sci. 5 (3), 335.

Fooladi, A.I., Tavakoli, H., Naderi, A., 2010. Detection of enterotoxigenic Staphylococcus aureus isolates in domestic dairy products. Iran. J. Microbiol. 2 (3), 137.

Gao, Z., Chao, F., Chao, Z., Li, G., 2000. Detection of staphylococcal enterotoxin C2 employing a piezoelectric crystal immunosensor. Sens. Actuators B: Chem. 66 (1), 193–196.

Gholamzad, M., Khatami, M.R., Ghassemi, S., Malekshahi, Z.V., Shooshtari, M.B., 2015. Detection of staphylococcus enterotoxin B (SEB) using an immunochromatographic test strip. Jundishapur J. Microbiol. 8 (9).

Gupta, G., Singh, P.K., Boopathi, M., Kamboj, D., Singh, B., Vijayaraghavan, R., 2010a. Molecularly imprinted polymer for the recognition of biological warfare agent staphylococcal enterotoxin B based on surface plasmon resonance. Thin Solid Films 519 (3), 1115–1121.

Gupta, G., Singh, P.K., Boopathi, M., Kamboj, D., Singh, B., Vijayaraghavan, R., 2010b. Surface plasmon resonance detection of biological warfare agent Staphylococcal enterotoxin B using high affinity monoclonal antibody. Thin Solid Films 519 (3), 1171–1177.

Hajihosseini, S., Nasirizadeh, N., Hejazi, M.S., Yaghmaei, P., 2016. A sensitive DNA biosensor fabricated from gold nanoparticles and graphene oxide on a glassy carbon electrode. Mater. Sci. Eng.: C 61, 506–515.

Hedayati, Ch.M., Amani, J., Sedighian, H., Amin, M., Salimian, J., Halabian, R., Imani Fooladi, A.A., 2016. Isolation of a new ssDNA aptamer against staphylococcal enterotoxin B based on CNBr-activated sepharose-4B affinity chromatography. J. Mol. Recognit. 29 (9), 436–445.

Huang, Y., Zhang, H., Chen, X., Wang, X., Duan, N., Wu, S., Xu, B., Wang, Z., 2015. A multicolor time-resolved fluorescence aptasensor for the simultaneous detection of multiplex Staphylococcus aureus enterotoxins in the milk. Biosens. Bioelectron. 74, 170–176.

Imani-Fooladi, A.A., Yousefi, F., Mousavi, S.F., Amani, J., 2014. In silico design and analysis of TGFαl3-seb fusion protein as “a new antitumor agent” candidate by ligand-targeted superantigens technique. Iran. J. Cancer Prev. 7 (3), 152.

Imani Fouladi, A., Choupani, A., Fallah Mehrabadi, J., 2011. Study of prevalence of enterotoxin type B gene in meticillin resistant Staphylococcus aureus (MRSA) isolated from wound. Kowsar Med. J. 16 (1), 21–25.

Justino, C.I., Freitas, A.C., Pereira, R., Duarte, A.C., Santos, T.A.R., 2015. Recent developments in recognition elements for chemical sensors and biosensors. TrAC Trends Anal. Chem. 68, 2–17.

Kientz, C.E., Hulst, A.G., Wils, E.R., 1997. Determination of staphylococcal enterotoxin B by on-line (micro) liquid chromatography-electrospray mass spectrometry. J. Chromatogr. A 757 (1–2), 51–64.

Liu, N., Li, X., Ma, X., Ou, G., Gao, Z., 2014. Rapid and multiple detections of staphylococcal enterotoxins by two-dimensional molecularly imprinted film-coated QCM sensor. Sens. Actuators B: Chem. 191, 326–331.

Luo, P., Liu, Y., Xia, Y., Xu, H., Xie, G., 2014. Aptamer biosensor for sensitive detection of toxin A of Clostridium difficile using gold nanoparticles synthesized by Bacillus stearothermophilus. Biosens. Bioelectron. 54, 217–221.

MEDINA, M.B., 2003. Detection of staphylococcal enterotoxin B (SEB) with surface plasmon resonance biosensor. J. Rapid Methods Autom. Microbiol. 11 (3), 225–243.

Medina, M.B., 2006. A biosensor method for detection of Staphylococcal enterotoxin A in raw whole egg. J. Rapid Methods Autom. Microbiol. 14 (2), 119–132.

Mello, P.L., Moraes Riboli, D.F., Pinheiro, L., de Almeida Martins, L., Vasconcelos Paiva Brito, M.A., Ribeiro de Souza da Cunha, Md.L., 2016. Detection of enterotoxigenic potential and determination of clonal profile in Staphylococcus aureus and coagulase-negative staphylococci isolated from bovine subclinical mastitis in different Brazilian states. Toxins 8 (4), 104.

Nasirizadeh, N., Zare, H.R., Pournaghi-Azar, M.H., Hejazi, M.S., 2011. Introduction of hematoxylin as an electroactive label for DNA biosensors and its employment in detection of target DNA sequence and single-base mismatch in human papilloma virus corresponding to oligonucleotide. Biosens. Bioelectron. 26 (5), 2638–2644.

Nedelkov, D., Nelson, R.W., 2003. Detection of staphylococcal enterotoxin B via biomolecular interaction analysis mass spectrometry. Appl. Environ. Microbiol. 69 (9), 5212–5215.

Pumera, M., 2010. Graphene-based nanomaterials and their electrochemistry. Chem. Soc. Rev. 39 (11), 4146–4157.

Pumera, M., 2011. Graphene in biosensing. Mater. Today 14 (7–8), 308–315.

Radi, A.-E., 2011. Electrochemical aptamer-based biosensors: recent advances and perspectives. Int. J. Electrochem. 2011.

Rasooly, A., 2001. Surface plasmon resonance analysis of staphylococcal enterotoxin B in food. J. Food Prot. 64 (1), 37–43.

Saadat, Y.R., Fooladi, A.A.I., Shapouri, R., Hosseini, M.M., Khiabani, Z.D., 2014. Prevalence of enterotoxigenic Staphylococcus aureus in organic milk and cheese in Tabriz, Iran. Iran. J. Microbiol. 6 (5), 345.

Sabri, Y.M., Kandjani, A.E., Ippolito, S.J., Bhargava, S.K., 2016. Ordered monolayer gold nano-urchin structures and their size induced control for high gas sensing performance. Sci. Rep. 6, 24625.

Salmain, M., Ghasemi, M., Boujday, S., Spadavecchia, J., Técher, C., Val, F., Le Moigne, V., Gautier, M., Briandet, R., Pradier, C.-M., 2011. Piezoelectric immunosensor for direct and rapid detection of staphylococcal enterotoxin A (SEA) at the ng level. Biosens. Bioelectron. 29 (1), 140–144.

Schotte, U., Langfeldt, N., Peruski, A.H., Meyer, H., 2002. Detection of staphylococcal enterotoxin B (SEB) by enzyme-linked immunosorbent assay and by a rapid handheld assay. Clin. Lab. 48 (7–8), 395–400.

Seifati, S.M., Nasirizadeh, N., Azimzadeh, M., 2018. Nano-biosensor based on reduced graphene oxide and gold nanoparticles, for detection of phenylketonuria-associated DNA mutation. IET Nanobiotechnol. 12 (4), 417–422.

Sharma, A., Kameswara Rao, V., Vrat Kamboj, D., Jain, R., 2014. Electrochemical immunosensor for staphylococcal enterotoxin B (SEB) based on platinum nanoparticles-modified electrode using hydrogen evolution inhibition approach. Electroanalysis 26 (11), 2320–2327.

Sharma, A., Rao, V.K., Kamboj, D.V., Gaur, R., Shaik, M., Shrivastava, A.R., 2016. Enzyme free detection of staphylococcal enterotoxin B (SEB) using ferrocene carboxylic acid labeled monoclonal antibodies: an electrochemical approach. New J. Chem. 40 (10), 8334–8341.

Shoaie, N., Forouzandeh, M., Omidfar, K., 2018a. Highly sensitive electrochemical biosensor based on polyaniline and gold nanoparticles for DNA detection. IEEE Sens. J. 18 (5), 1835–1843.

Shoaie, N., Forouzandeh, M., Omidfar, K., 2018b. Voltammetric determination of the Escherichia coli DNA using a screen-printed carbon electrode modified with polyaniline and gold nanoparticles. Microchim. Acta 185 (4), 217.

Shojaei, S., Nasirizadeh, N., Entezam, M., Koosha, M., Azimzadeh, M., 2016. An electrochemical nanosensor based on molecularly imprinted polymer (MIP) for detection of gallic acid in fruit juices. Food Anal. Methods 1–11.

Spindel, S., Balsam, J., Mattay, G., Sapsford, K.E., 2015. Investigating low volume planar surface fluorescent immunoassays with QDs for spatial and spectral multiplexing. Sens. Actuators B: Chem. 215, 396–404.

Syedmoradi, L., Daneshpour, M., Alvandipour, M., Gomez, F.A., Hajghassem, H., Omidfar, K., 2017. Point of care testing: the impact of nanotechnology. Biosens. Bioelectron. 87, 373–387.

Tang, D., Tang, J., Su, B., Chen, G., 2010. Ultrasensitive electrochemical immunoassay of staphylococcal enterotoxin B in food using enzyme-nanosilica-doped carbon nanotubes for signal amplification. J. Agric. Food Chem. 58 (20), 10824–10830.

Thapliyal, N.B., Chiwunze, T.E., Karpoormath, R., Cherukupalli, S., 2017. Fabrication of highly sensitive gold nanourchins based electrochemical sensor for nanomolar determination of primaquine. Mater. Sci. Eng.: C 74, 27–35.

Topkaya, S.N., Azimzadeh, M., 2016. Biosensors of in vitro detection of cancer and bacterial cells. Nanobiosensors for Personalized and Onsite Biomedical Diagnosis. Institution of Engineering and Technology, United Kingdom, pp. 73–94.

Wu, S., Duan, N., Gu, H., Hao, L., Ye, H., Gong, W., Wang, Z., 2016. A review of the methods for detection of Staphylococcus aureus enterotoxins. Toxins 8 (7), 176.

Wu, S., Duan, N., Ma, X., Xia, Y., Wang, H., Wang, Z., 2013. A highly sensitive fluorescence resonance energy transfer aptasensor for staphylococcal enterotoxin B detection based on exonuclease-catalyzed target recycling strategy. Anal. Chim. Acta 782, 59–66.

Xiong, X., Shi, X., Liu, Y., Lu, L., You, J., 2018. An aptamer-based electrochemical biosensor for simple and sensitive detection of staphylococcal enterotoxin B in milk. Anal. Methods.

Yang, M., Kostov, Y., Bruck, H.A., Rasooly, A., 2009. Gold nanoparticle-based enhanced chemiluminescence immunosensor for detection of staphylococcal enterotoxin B (SEB) in food. Int. J. Food Microbiol. 133 (3), 265–271.

Yazdanparast, S., Benvidi, A., Banaei, M., Nikukar, H., Tezerjani, M.D., Azimzadeh, M., 2018. Dual-aptamer based electrochemical sandwich biosensor for MCF-7 human breast cancer cells using silver nanoparticle labels and a poly (glutamic acid)/MWNT

nanocomposite. Microchim. Acta 185 (9), 405.
Zargar, M.H.S., Doust, R.H., Mobarez, A.M., 2014. Staphylococcus aureus enterotoxin A gene isolated from raw red meat and poultry in Tehran, Iran. Int. J. Enteric Pathog. 2 (3), e16085.
Zeleny, R., Emteborg, H., Charoud-Got, J., Schimmel, H., Nia, Y., Mutel, I., Ostyn, A., Herbin, S., Hennekinne, J.-A., 2015. Development of a reference material for Staphylococcus aureus enterotoxin A in cheese: feasibility study, processing, homogeneity and stability assessment. Food Chem. 168, 241–246.
Zhou, M., Zhai, Y., Dong, S., 2009. Electrochemical sensing and biosensing platform based on chemically reduced graphene oxide. Anal. Chem. 81 (14), 5603–5613.